Helices of Boron−Nitrogen Hexagons and Decagons. A Theoretical Study

Csaba E. Szakacs[†] and Paul G. Mezey*[,†,‡]

Scientific Modeling and Simulation Laboratory (SMSL), Department of Chemistry, and Department of Physics and Physical Oceanography, Memorial University of Newfoundland, St. John's, NL A1B 3X7, Canada, and Institute for Advanced Study, Collegium Budapest, Szentháromság utca 2, 1014 Budapest, Hungary

Received: March 29, 2008; Revised Manuscript Received: May 7, 2008

Ab initio self-consistent field molecular orbital and density functional theory calculations have been performed on a series of helical boron−nitrogen structures comprised of fused hexagons and larger polygons. The presence of an even number *N* of rings in the boron−nitrogen [*N*]helicenes leads to the possibility of angular isomers.[1] The electronic structure and stability of three isomeric nonhydrogenated boron−nitrogen helices were investigated at the HF/6-31G(d) and the B3LYP/6-31G(d) levels of theory. According to this study some of the initially assumed regular helical structures are unstable; two types of the isomeric structures convert to characteristically different equilibrium geometries. Electron density contours were calculated in order to interpret the existing bonding patterns.

I. Introduction

Following the discovery of fullerene[2] and carbon nanotubes,[3] theoretical studies in the early 1990s were already predicting the existence of their boron−nitrogen analogues.[4–6] The synthesis[7]of boron-nitride nanotubes (BNNTs) and later the experimental evidence[8,9] for the first boron−nitrogen fullerene-like structures justified their structural characterization. These fully boron-nitrogen nanocompounds proved to have high chemical and thermal stability.[10] Recently, the synthesis of novel boron−nitride helical conical nanotubes (BN HCNTs), having elastic properties was also reported.[11] Because of all these electronic, thermal, and mechanical properties, structures formed exclusively from boron and nitrogen could provide new options for novel materials with applications in nanotechnology. As a consequence, the theoretical study of the structure, stability, and electronic and other properties of fully boron−nitrogen compounds is attracting considerable interest.[12–18]

A recent theoretical study[1] investigated the structure and stability of some boron−nitrogen analogues of more extended polyhelicenic hydrogenated helices, providing some additional information on extended boron−nitrogen compounds.

In the quoted study it was observed that, in the case of boron−nitrogen analogues of helicenes, depending on the actual arrangements of the boron and nitrogen atoms in the terminal ring, an even number of *N* fused rings leads to the existence of relatively stable angular isomers, shown in Scheme 1. According to our notations, the two isomers are distinguished as follows: on the left-hand side the structures are called **NB**-type helices, and the right-hand side structures are called **BN**-type helices, respectively.

In the present paper further computational investigations are reported for a series of nonhydrogenated boron−nitrogen helices, formed by an even number *N* of fused boron−nitrogen hexagons and larger polygons. The two types of initially assumed helical structures, **NB** and **BN**, convert to characteristically different equilibrium geometries, depicted in Figure 1. The **NB** isomers have stable forms as helices **1**−**4** with 6, 8, 10, and 12 fused hexagons. The initially assumed helical **BN** isomers of hexagonal units, however, will suffer ring opening at the terminal rings, leading to helices **5**−**8**, with 2, 4, 6, and 8 fused hexagons and 2 terminal decagons, respectively. Interchanging again the positions of B and N atoms in the latter **BN**-type helices leads to additional isomers **9**−**12**. The geometrical structures, bond lengths, and energies of all these structures were compared for a better understanding of their relative stability, as such helices may become building blocks for more extended novel, somewhat flexible nanostructures.

TABLE 1: Calculated Lowest Vibrational Frequencies (cm^{-1}) of the Studied Boron−Nitrogen Helices 1−12

	frequencies	
helix	HF/6−31G(d)	B3LYP/6−31G(d)
1	40.5976	37.5390
2	29.5098	18.3546
3	34.9183	31.9349
4	33.0155	31.4745
5	19.8010	9.6610
6	16.5525	15.3029
7	21.1482	18.0346
8	25.3061	22.6926
9	13.0059	15.0621
10	17.0033	17.1246
11	17.5390	17.0579
12	18.4992	16.6334

II. Computational Methodology

Optimization calculations were performed for a number of nonhydrogenated boron−nitrogen helices. The levels of theory used were HF and B3LYP with the 6-31G(d) basis set.[19,20] All these methods are implemented in the Gaussian 03 software package.[21] For verification of the energy minima for all optimized geometries, harmonic vibrational frequencies were computed at the same level of theory, and zero-point energy calculations were also carried out. Electron density analysis was performed for some of the structures using DFT, with the B3LYP functional and 6-31G(d) basis set, for the purpose of

* To whom correspondence should be addressed. Phone: (709)737-6118. Fax: (709)737-3702. E-mail: paper.mezey@gmail.com.
† Memorial University of Newfoundland.
‡ Collegium Budapest.

10.1021/jp802722p CCC: $40.75
Published on Web 06/28/2008

SCHEME 1: The Two Types of Nonhydrogenated Boron−Nitrogen Angular Helices NB and BN in the Case of Six Fused Hexagons

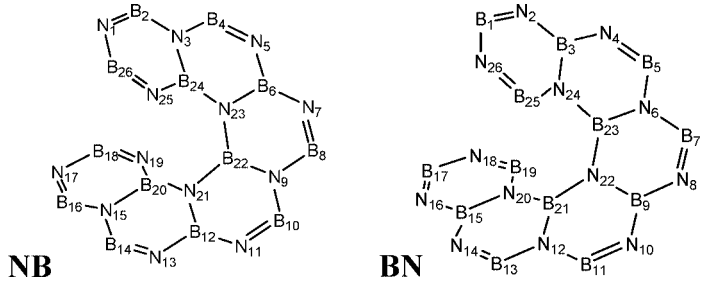

TABLE 2: Calculated Total Energies (TE, in Hartree), Relative Energies[a] (ΔE, in kcal/mol), Sum of Total and Zero-Point Vibrational Energies (TE + ZPVE, in Hartree), and Relative Energies Including ZPVE ($\Delta E_{TE+ZPVE}$, in kcal/mol) for Boron−Nitrogen Helices 1−12

	HF/6-31G(d)				B3LYP/6-31G(d)			
molecule	TE	ΔE	TE+ZPVE	$\Delta E_{TE+ZPVE}$	TE	ΔE	TE+ZPVE	$\Delta E_{TE+ZPVE}$
1	−1029.4354	88.4	−1029.3026	89.4	−1035.4972	77.3	−1035.3734	77.7
2	−1346.2350	86.3	−1346.0600	87.3	−1354.1588	75.0	−1353.9958	75.4
3	−1663.0285	90.0	−1662.8113	91.0	−1672.8160	77.5	−1672.6135	77.9
4	−1979.8189	91.7	−1979.5597	92.6	−1991.4709	78.9	−1991.2292	79.2
5	−1029.5763	0.0	−1029.4450	0.0	−1035.6203	0.0	−1035.4973	0.0
6	−1346.3726	0.0	−1346.1992	0.0	−1354.2783	0.0	−1354.1159	0.0
7	−1663.1719	0.0	−1662.9562	0.0	−1672.9395	0.0	−1672.7377	0.0
8	−1979.9651	0.0	−1979.7073	0.0	−1991.5966	0.0	−1991.3554	0.0
9	−1029.5784	−1.3	−1029.4471	−1.3	−1035.6228	−1.6	−1035.4997	−1.5
10	−1346.3698	1.7	−1346.1963	1.8	−1354.2775	0.5	−1354.1150	0.5
11	−1663.1632	5.5	−1662.9477	5.4	−1672.9343	3.3	−1672.7326	3.2
12	−1979.9536	7.2	−1979.6961	7.0	−1991.5893	4.6	−1991.3485	4.4

[a] All relative energy values are calculated in comparison to the set of helices **5**−**8**, for which a relative energy of zero is assigned.

obtaining additional information helping to understand the bonding pattern in these systems.

III. Results and Disscussion

Geometries and Bond Lengths. The optimized geometries of all the boron−nitrogen structures **1**−**12** are shown in Figure 1. Note that, all the optimized structures have helicoidal geometry, except compound **5**, which is a partial helix, and compound **9**, which prefers a planar conformation. All the optimized structures are characterized to be minima by having real vibrational frequencies. The calculated lowest vibrational frequencies, corresponding to primarily spring-like motions of the helical systems, are shown in Table 1. The facility of such distorsions is an indication of the potential application of these units in flexible nanostructures.

For the nonterminal rings of helices **1**−**4**, there are essentially four kinds of boron−nitrogen bond lengths denoted *j*, *k*, *l*, and *m* (Figure 2). Whereas the two bond lengths *j* and *k* tend to be larger, the bond length *m* is shorter, indicating bonds that are stronger at the peripheries of the helices. The two end-rings show major deviations when compared to the inner units of the helices.

The final optimized structures **5**−**12** show a ring opening at the two original terminal hexagons, leading to the formation of boron−nitrogen decagons at both ends. This ring opening tendency may be partly due to the boron atoms preference for a linear bond system when placed between two nitrogen atoms.

The four bond types denoted by *j*, *k*, *l*, and *m*, observed in helices **1**−**4**, are characteristic for the inner hexagons of helices **5**−**12** as well. However, for the terminal rings of structures **5**−**12**, nine types of boron−nitrogen bond lengths can be observed, denoted by *a*, *b*, *c*, *d*, *e*, *f*, *g*, *h*, and *i* (Figures 3 and 4). The corresponding bond lengths in the two decagons have the same values at both ends in all the structures, due to symmetry.

Investigating the bond lengths in the terminal polygon in each case (**5**−**12**), one can conclude that these bonds are consistently strong, much stronger than bond types *k* and *j*.

Electron Density Analysis. Electron density calculations were performed for the helices **2**, **6**, and **10**, as well as for the largest optimized structures **4**, **8**, and **12**, using density functional theory. The detailed electron density shape analyses of these molecules (Figure 5) provide a justification, and are in strong agreement with the bond length considerations. The shape analysis shows a higher level of electron density distribution in the terminal rings (being decagons in helices **6**, **8**, **10**, and **12**, and hexagons in helices **2** and **4**) as well as along the peripheries for all the helices, where the alternating pattern due to the alternation of boron and nitrogen atoms is well manifested. This electron density enrichment in the terminal and peripheral regions is probably due to the tendency of even partial π systems for allowing electron repulsion to enhance arrangements with accumulations of electrons far apart, resulting in stronger bonds in the terminal rings and peripheries, respectively.

Looking at the nonterminal rings, especially where both the boron and the nitrogen atoms are trivalent, there is a depletion in the electron density (shown as discontinuity in the actual 0.20 a.u. electron density contours). This fact is also manifested in larger bond lengths in the inner hexagons.

Energies. In all three types of helices, as the number of fused rings increases, a nearly exactly linear decrease in the total energy is observed (Table 2).

Helices **5**−**8** are energetically more stable than helices **1**−**4**. The ring opening and formation of decagons at the two terminal

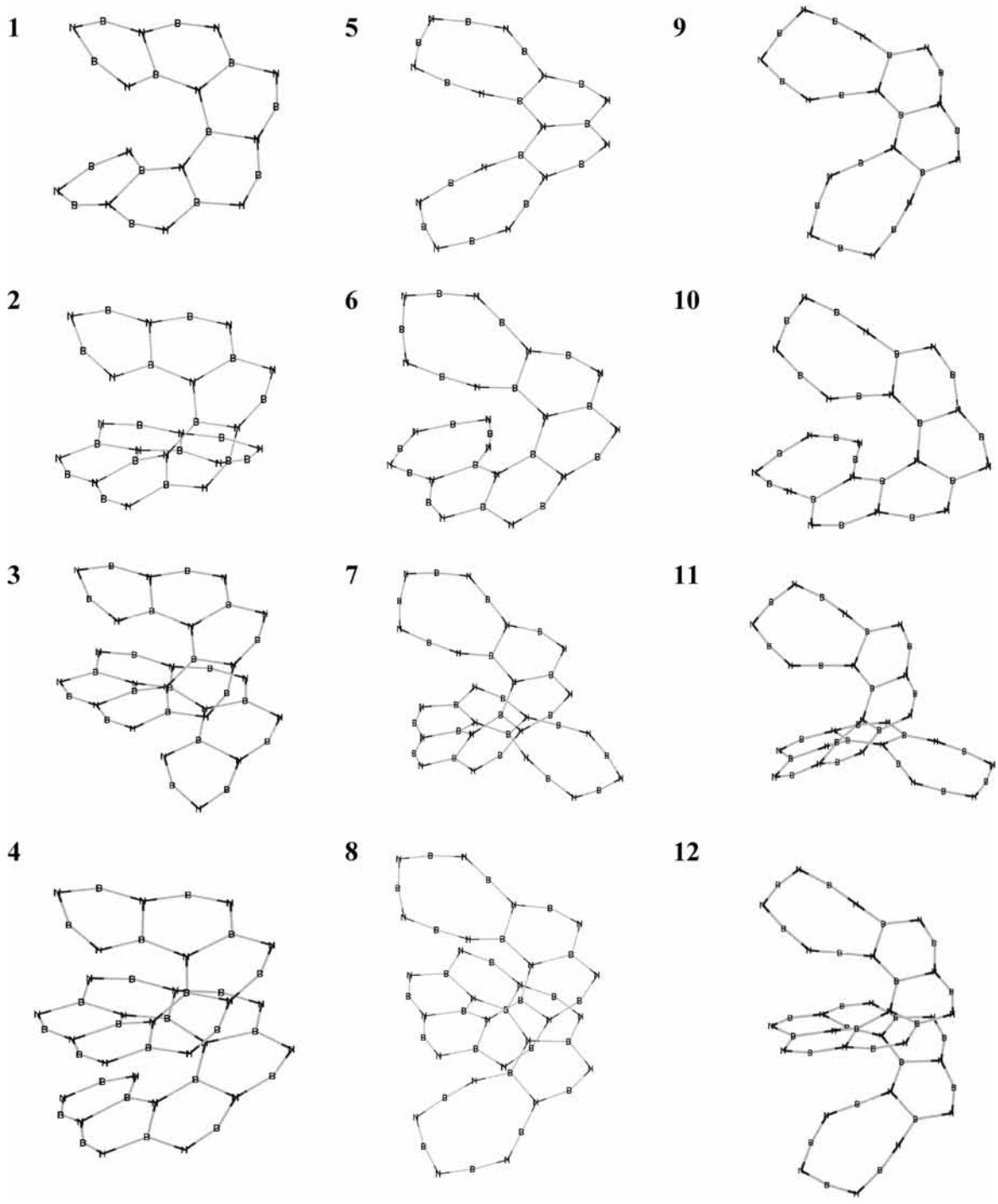

Figure 1. The optimized geometries of structures **1**−**12** at the B3LYP/6-31G level of theory.

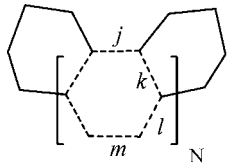

	1 (N=4)	**2** (N=6)	**3** (N=8)	**4** (N=10)
j=	1.449-1.452	1.444-1.468	1.442-1.461	1.446-1.462
k=	1.552-1.664	1.550-1.661	1.550-1.652	1.549-1.649
l=	1.376-1.444	1.372-1.447	1.376-1.444	1.374-1.445
m=	1.279-1.282	1.279-1.284	1.278-1.283	1.277-1.286

Figure 2. Bond lengths (in angstroms) at the B3LYP/6-31G level of theory for helices **1**, **2**, **3**, and **4**. The N in the schematic representation of the structures represents the number of inner hexagons.

rings seem to enhance their stability. The difference in the relative energy values between the two types of helices ranges between 88.4 and 91.7 kcal/mol at the HF/6-31G(d) level, and between 75.0 and 78.9 kcal/mol at the B3LYP/6-31G(d) level. The inclusion of ZPVE correction in estimating the relative energies does not modify the ordering and the considerable differences between isomers (Table 2).

When comparing the **5**−**8**-type helices to their **9**−**12** counterparts, it should be noted that, because of the planar conformation in the final optimized geometry, structure **9** is lower in

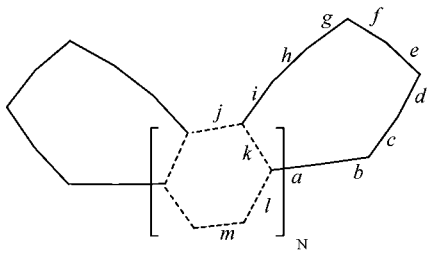

	5 (N=2)	**6** (N=4)	**7** (N=6)	**8** (N=8)
a=	1.363	1.362	1.365	1.366
b=	1.297	1.297	1.294	1.294
c=	1.338	1.337	1.338	1.338
d=	1.318	1.319	1.318	1.318
e=	1.349	1.348	1.347	1.346
f=	1.319	1.320	1.321	1.323
g=	1.358	1.357	1.353	1.352
h=	1.289	1.290	1.293	1.294
i=	1.372	1.380	1.378	1.378
j=	1.465	1.451-1.457	1.445-1.459	1.446-1.461
k=	1.568-1.600	1.554-1.591	1.551-1.592	1.551-1.587
l=	1.384-1.445	1.375-1.448	1.374-1.452	1.377-1.448
m=	1.278	1.277-1.282	1.279-1.284	1.278-1.285

Figure 3. Bond lengths (in angstroms) at the B3LYP/6-31G level of theory for helices **5**, **6**, **7**, and **8**. The number N in the schematic representation of the structures represents the number of inner hexagons.

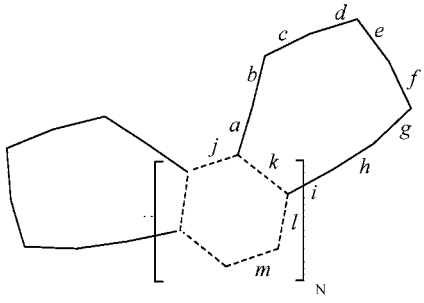

	9 (N=2)	**10** (N=4)	**11** (N=6)	**12** (N=8)
a=	1.375	1.374	1.373	1.373
b=	1.298	1.300	1.300	1.300
c=	1.336	1.338	1.337	1.337
d=	1.319	1.318	1.319	1.319
e=	1.349	1.349	1.349	1.349
f=	1.321	1.321	1.321	1.321
g=	1.358	1.358	1.359	1.359
h=	1.290	1.290	1.290	1.290
i=	1.375	1.375	1.376	1.376
j=	1.448	1.448-1.452	1.449-1.455	1.448-1.455
k=	1.521-1.621	1.529-1.614	1.529-1.614	1.532-1.616
l=	1.386-1.439	1.382-1.441	1.380-1.439	1.380-1.439
m=	1.279	1.279-1.281	1.279-1.281	1.279-1.281

Figure 4. Bond lengths (in angstroms) at the 6-31G(d)/B3LYP level of theory for helices **9**−**12**. The N in the schematic representation of the structures represents the number of inner hexagons.

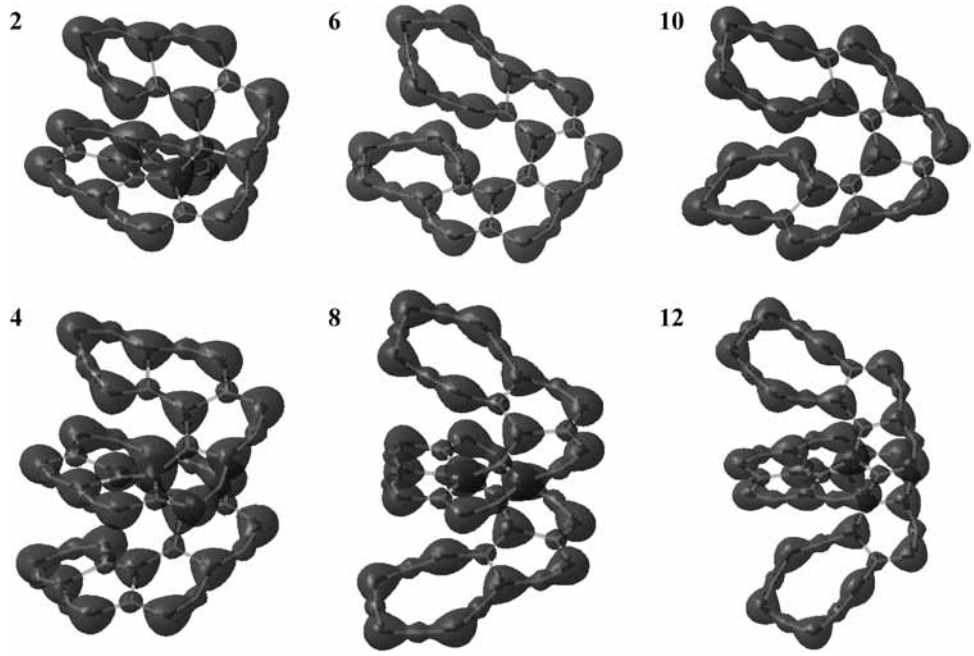

Figure 5. Electron density isocontours of helices **2** (with eight fused hexagons), **6**, and **10** (with four fused hexagons and two terminal decagons) at 0.20 a.u.

energy than the partial helix **5**, by approximately 1.3 kcal/mol at the HF/6-31G(d) level and by approximately 1.5 kcal/mol at the B3LYP/6-31G(d) level of theory (Table 2).

However, the fully helicoidal structures **10**, **11**, and **12** are higher in energy than helices **6**, **7**, and **8**, by approximately 1.7, 5.5, and 7.2 kcal/mol at the HF/6-31G(d) level of theory and

by 0.8, 3.3, and 4.6 kcal/mol at the B3LYP/6-31G(d) level of theory, respectively.

IV. Summary

The initially assumed helical **BN** isomers of hexagonal units suffer a ring opening in the terminal rings, due to the boron atom's preference for linearity. Comparing the energy values of the fully optimized ground states, it can be concluded that the ring opening causes a stabilization of the helices containing terminal decagon rings. Alternating again the boron and nitrogen atoms in these helices, new, relatively stable isomers are obtained. In the present study, attention was given to the stability, geometry, bonding pattern, and energies of these helices, as such molecules could provide useful information in the quest for novel materials based fully on boron and nitrogen. These structures are rather flexible and behave like "nano-springs", suggesting new possibilities, and may become models toward the synthesis of new, helical boron-nitrides.

Acknowledgment. This study has been supported by the Natural Sciences and Engineering Research Council of Canada, the Scientific Modeling and Simulation Laboratory (SMSL), and the Advanced Computation and Visualization Center of Memorial University of Newfoundland. Additional thanks are due to the Atlantic Computational Excellence Network (ACEnet) for computer resources, as well as to the Institute for Advanced Study, Collegium Budapest.

References and Notes

(1) Szakacs, C. E.; Mezey, P. G. *J. Phys. Chem. A* **2008**, *112* (11), 2477.

(2) Kroto, H. W.; Heath, J. R.; O'Brien, S. C.; Curl, R. F.; Smalley, R. E. *Nature* **1985**, *318*, 162.

(3) Iijima, S *Nature* **1991**, *354*, 56.

(4) Xia, X.; Jelski, D. A.; Bowser, J. R.; George, T. F. *J. Am. Chem. Soc.* **1992**, *114* (16), 6493.

(5) Silaghi-Dumitrescu, I.; Haiduc, I; Sowerby, D. B. *Inorg. Chem.* **1993**, *32* (17), 3755.

(6) Rubio, A.; Corkill, J. L.; Cohen, M. L. *Phys. Rev. B* **1994**, *49*, 5081.

(7) Chopra, N. G.; Luyken, R. J.; Cherrey, K.; Crespi, V. H.; Cohen, M. L.; Louie, S. G.; Zettl, A. *Science* **1995**, *269*, 966.

(8) Stephan, O.; Bando, Y.; Loiseau, A.; Willaime, F.; Shramchenko, N.; Tamiya, T.; Sato, T. *Appl. Phys. A: Mater. Sci. Process.* **1998**, *67*, 107.

(9) Golberg, D.; Bando, Y.; Stephan, O.; Kurashima, K. *Appl. Phys. Lett.* **1998**, *73*, 2441.

(10) Han, W. Q.; Mickelson, W.; Cumings, J.; Zettl, A. *Appl. Phys. Lett.* **2002**, *81*, 1110.

(11) Xu, F. F.; Bando, Y.; Ma, R.; Golberg, D.; Li, Y.; Mitome, M. *J. Am. Chem. Soc.* **2003**, *125*, 8032.

(12) Seifert, G.; Fowler, P. W.; Mitchell, D.; Porezag, D.; Frauenheim, T. *Chem. Phys. Lett.* **1997**, *268*, 352.

(13) Kongsted, J.; Osted, A.; Jensen, L.; Astrand, P.-O.; Mikkelsen, K. V. *J. Phys. Chem. B* **2001**, *105*, 10243.

(14) Strout, D. L. *Chem. Phys. Lett.* **2004**, *383*, 95.

(15) Silaghi-Dumitrescu, I.; Lara-Ochoa, F.; Bishof, P.; Haiduc, I. *J. Mol. Struct. (THEOCHEM)* **1996**, *367*, 47.

(16) Wu, H. S.; Cui, X. Y.; Xu, X. H. *J. Mol. Struct. (THEOCHEM)* **2005**, *717*, 107.

(17) Xu, S.; Zhang, M.; Zhao, Y.; Chen, B.; Zhang, J.; Sun, C. *Chem. Phys. Lett.* **2006**, *418*, 297.

(18) Batista, R. J. C.; Mazzoni, M. S. C.; Chacham, H. *Chem. Phys. Lett.* **2006**, *421*, 246.

(19) Becke, A. D. *J. Chem. Phys.* **1993**, *98*, 5648–5652.

(20) Lee, C.; Yang, W.; Parr, R. G. *Phys. Rev. B* **1988**, *37*, 785–787.

(21) Frisch, M. J.; Trucks, G. W.; Schlegel, H. B.; Scuseria, G. E.; Robb, M. A.; Cheeseman, J. R.; Montgomery, J. A., Jr.; Vreven, T.; Kudin, K. N.; Burant, J. C.; Millam, J. M.; Iyengar, S. S.; Tomasi, J.; Barone, V.; Mennucci, B.; Cossi, M.; Scalmani, G.; Rega, N.; Petersson, G. A.; Nakatsuji, H.; Hada, M.; Ehara, M.; Toyota, K.; Fukuda, R.; Hasegawa, J.; Ishida, M.; Nakajima, T.; Honda, Y.; Kitao, O.; Nakai, H.; Klene, M.; Li, X.; Knox, J. E.; Hratchian, H. P.; Cross, J. B.; Bakken, V.; Adamo, C.; Jaramillo, J.; Gomperts, R.; Stratmann, R. E.; Yazyev, O.; Austin, A. J.; Cammi, R.; Pomelli, C.; Ochterski, J. W.; Ayala, P. Y.; Morokuma, K.; Voth, G. A.; Salvador, P.; Dannenberg, J. J.; Zakrzewski, V. G.; Dapprich, S.; Daniels, A. D.; Strain, M. C.; Farkas, O.; Malick, D. K.; Rabuck, A. D.; Raghavachari, K.; Foresman, J. B.; Ortiz, J. V.; Cui, Q.; Baboul, A. G.; Clifford, S.; Cioslowski, J.; Stefanov, B. B.; Liu, G.; Liashenko, A.; Piskorz, P.; Komaromi, I.; Martin, R. L.; Fox, D. J.; Keith, T.; Al-Laham, M. A.; Peng, C. Y.; Nanayakkara, A.; Challacombe, M.; Gill, P. M. W.; Johnson, B.; Chen, W.; Wong, M. W.; Gonzalez, C.; Pople, J. A. *Gaussian 03*, revision C.02; Gaussian, Inc.: Wallingford, CT, 2004.

JP802722P